DOI 10.1007/s10812-016-0318-x
Journal of Applied Spectroscopy, Vol. 83, No. 3, July, 2016 (Russian Original Vol. 83, No. 3, May–June, 2016)

OPTIMIZATION OF CONDITIONS FOR DETERMINATION OF Cr AND Ni IN STEEL BY THE METHOD OF LASER-INDUCED BREAKDOWN SPECTROSCOPY WITH THE USE OF PARTIAL LEAST SQUARES REGRESSION

M. Singh, V. Karki, and A. Sarkar*

UDC 533.9;621.373.8

The effect of laser energy and acquisition time delay on the overall analytical performance of laser-induced breakdown spectroscopy (LIBS) analyses for Cr and Ni in steel samples is evaluated. The analyses were carried out by using the partial least squares regression (PLSR) algorithm. The optimum analytical condition for analysis based on the signal-to-noise ratio (SNR) was found to be nearly the same for both elements. Five additional experimental conditions using different combinations of laser energy and acquisition time delay were also used for the LIBS studies. The least standard error of prediction was obtained at the optimal experimental conditions based on best SNR (90–95 mJ of laser energy with 1.1–1.3 μs acquisition time delay). With deviation from the optimum condition in either laser energy or acquisition time delay axis, the error in prediction increases, indicating a poorer analytical performance for both Cr and Ni.

Keywords: *laser-induced breakdown spectroscopy, optimization conditions, optimum parameters, partial least squares regression.*

Introduction. Laser-induced breakdown spectroscopy (LIBS) is an emerging technique for material characterization, which is rapidly maturing and is commonly accepted as an essential tool in analytical chemistry. From the day of the first report of the laser-induced plasma by G. C. Dacey in 1962 to the present day, the umbrella of LIBS has spread in numerous fields, including underwater and space explorations [1–3]. A number of review articles discussing the pros and cons of LIBS are available [4, 5]. The most important advantage of LIBS is its ability to simultaneously analyze all elements of the Periodic Table in any form or matrix (gas, liquid, or solid) [6, 7]. Recently, the nuclear industry is also looking at LIBS, as it can give real time and remote information on samples, which is an essential requirement in the radioactive field [8, 9].

Even though LIBS has many advantages over the commonly used techniques like inductively coupled plasma-mass spectrometry/optical emission spectrometry (ICP-MS/OES), thermal ionization mass spectrometry (TIMS), neutron activation analysis (NAA), etc., the relative accuracy and precision for LIBS in a complex system have been a point of concern. For LIBS, being an optical emission technique, the selection of emission lines is the governing factor for achieving superior analytical performance. An emission line with high signal-to-noise ratio and good spectral purity leads to better analytical results. Selection of such emission line is a difficult task, especially for a sample of high complexity containing many elements. In such a situation, the strongest emission line often lacks spectral purity, hence not so strong emission lines but having sufficient signal-to-noise ratio, are chosen for the LIBS study.

In order to improve the analytical performance of the LIBS system, apart from the selection of appropriate emission lines, one needs to correct or optimize some key analytical parameters of the experimental setting. The parameters that mostly affect LIBS measurements include the laser properties (laser energy, wavelength, and pulse duration), lens to sample distance (focusing parameter), sample property (i.e., matrix effect), plasma environment, and the temporal detection window, which includes acquisition time delay and gate width. The most important parameters of the above that are optimized in a LIBS study are laser energy and acquisition time delay [10, 11]. The interaction between the laser light and the sample is a complex process and is out of the scope of the present manuscript [12]. In short, the evolution of the laser-induced plasma can be divided into several transient phases depending on the emitting species. The early stage of the plasma is dominated by a continuum background emission due to the Bremsstrahlung and recombination reactions in the plasma. The continuum

*To whom correspondence should be addressed.

Fuel Chemistry Division, Bhabha Atomic Research Centre, Mumbai 400 085, India; e-mail: arnab@barc.gov.in.
Abstract of article is published in Zhurnal Prikladnoi Spektroskopii, Vol. 83, No. 3, p. 501, May–June, 2016.

background decays rapidly with time with respect to the decay of the emission line signal. A properly selected acquisition delay for detection improves the signal of interest from the continuum emission. Since noise depends on the intensity magnitude, and high continuum emission corresponds to high noise. Too much delay may cause a decrease in the signal to the extent that it becomes irrelevant for any practical analytical purpose. On the other hand, the signal and the continuum (hence the corresponding noise) in any time window increases with increasing laser energy, but the increase in signal is higher than the noise increase and thereby influences more effectively the signal-to-noise ratio. With very high laser energy, plasma shielding starts to block the laser light from reaching the sample surface. As a result, the analytical signal begins to decrease, causing a reduction in the signal-to-noise ratio [3, 13].

Usually, one variable at a time is used when optimizing an experimental parameter while monitoring the signal-to-noise or signal-to-background ratios as figure of merit [14]. The signal-to-noise ratio is typically more effective than the signal-to-background ratio since at very low laser energy or at very high acquisition delay the magnitude of background often falls close to zero, which results in a very high signal-to-background ratio. However, this cannot be an optimum condition for the analysis. For the optimization, the acquisition time delay (or laser energy) is fixed to an arbitrarily chosen value, and the laser energy (or acquisition time delay) is varied to determine the maximum signal-to-noise ratio. While maintaining the laser energy (or acquisition time delay) fixed at a previously optimized value, the acquisition time delay (or laser energy) is now varied and optimized. For the optimization study in our laboratory, we employed a simultaneous optimization of all variables [9, 13]. In this technique, both the independent parameters, laser energy and acquisition time delay, are simultaneously varied to monitor the signal-to-noise ratio and a three-dimensional plot of the laser energy vs. acquisition time delay vs. signal-to-noise ratio is created to find the best signal-to-noise ratio condition. In the case of a simultaneous multiple elemental analyses, an average condition selected from the individually optimized conditions for selected elements is chosen [13, 15].

In this study, efforts were focused on the effect of different experimental conditions in regards to the analytical performance of the LIBS analysis. Chromium and Ni in stainless steel were determined using the partial least squares regression (PLSR) algorithm. The analytical performances of the PLSR results were compared on the basis of a statistical parameter, standard error of predictions (SEP). Six different experimental conditions were used for evaluating the effect of experimental conditions on the analytical performance of the LIBS analysis.

Experimental. *LIBS system and measurements.* A lab assembled LIBS system has been used in the present study. A frequency doubled (532 nm), Nd:YAG laser (Brilliant B, Quantel, France) was used. Its beam of 6 ns pulse duration was focused using a plano-convex lens to produce the laser induced plasma. The lens to sample distance was 24.8 cm. The plasma emission was collected through a collimator placed at a distance of 6 cm and an angle of 45^{o} with respect to the incident laser beam. The collimator is a light collection system consisting of quartz lens and mirrors (CC52, Andor, UK), and the plasma plume produced was imaged onto a high-resolution echelle spectrometer (Mechelle, ME5000, Andor, UK) slit by using an optical fiber. The spectrograph (195 mm focal length) covers the 200–975 nm wavelength range in one setting with a constant spectral resolution ($\lambda/\Delta\lambda$) of ~5000 at 10 μm slit width. The spectrograph was attached with an intensifier charge coupled device (iStar, Andor, UK) embedded with a delay generator. The detector was in synchronization with the laser pulse Q-switch to control the acquisition time delay and gate width. Intensity and wavelength calibrations of the spectrograph-intensifier charge coupled device were carried out using NIST certified deuterium-quartz-tungsten-halogen (DH2000, Ocean Optics, USA) and Hg–Ar (HG-1, Ocean Optics, USA) lamps, respectively. The samples were placed on an XYZ-translator (Velmex, USA). Laser pulse energy was measured with a pre-calibrated energy meter (Ophire Photonics, Israel).

Analysis: For every LIBS spectrum, 50 shots at a certain position were accumulated. The detector gate width was fixed at 20 μs. The gain of the intensifier charge coupled device was set at 2500 (out of a maximum setting of 4096). Since the readout time of the intensifier charge coupled device was of ~0.5 s, one Hz frequency laser was used to avoid any loss of data. Ten certified high alloy steel samples, provided by Federal Institute for Materials Research and Testing, Germany (BAM), in the framework of the LIBS 2008 contest were used. The compositions of Cr and Ni in the samples were provided by BAM (Table 1). The choice of the multivariate regression method like PLSR instead of a simple least square regression was based on the superiority of the multivariate methods over simple univariate methods reported in [16, 17]. An important criterion for using a simple univariate regression to achieve good analytical data is to have sufficient spectral emission lines with high spectral clarity. For a complex system like steel, the majority of elemental peaks are only partially resolved. In such scenario, multivariate analysis like PLSR is a more accurate approach for quantitative analysis. For a statistical comparison of the spectra, the samples was arranged in two groups or sets before performing PLSR. A calibration set consisting of seven samples was used for constructing calibration curves using the PLSR algorithm, and a validation set consisting of three

TABLE 1. Certified Composition of Steel Samples for Cr and Ni

Sample	Elemental concentration, wt.%	
	Ni	Cr
C1	12.55	12.35
C2	6.124	14.727
C3	12.85*	11.888
C4	10.2*	18.46*
C5	20.05	25.39
C6	9.24	17.31
C7	10.2	17.84
C8	8.9*	17.96
C9	5.66	14.14*
C10	10.72	16.811*

*The samples used for the validation set.

samples was used to validate the calibration models generated by PLSR. Each sample was analyzed 10 times, and these spectra were used in analysis. A PLSR routine was used to match the unknown sample's spectrum to the reference model spectra. PLSR was applied as a progressive approach that takes into account the intensity of each pixel. A detailed description of PLSR can be found in [18, 19]. The statistical parameter SEP was used to compare the analytical performance of the LIBS analyses [16].

$$SEP = \sqrt{\frac{1}{N-1}\sum_{i=0}^{N}\left(Y_s - Y_p\right)^2}, \quad (1)$$

where N is the total number of validation set samples ($N = 3$ in the present case), and Y_s and Y_p are the standard and predicted concentrations, respectively of the i^{th} validation set. The PLSR analysis was carried out using Unscrambler X (M/s Camo software, India) multivariate analysis software. A separate regression for Cr and Ni was carried out. For all the steel samples, the region of 670–975 nm has almost no significant observable signal, and hence only the 210–670 nm region was used for the PLSR calibration.

Results and Discussion. *Selection of line of interest.* As discussed previously, the two analytical parameters that are optimized prior to the LIBS analysis are laser energy and acquisition time delay, considering the signal-to-noise ratio as a figure of merit. Initially, all the detectable emission lines of Cr and Ni in steel are tabulated comparing the spectra with the Kurucz database [20]. Among these lines, only those lines that are found to be spectrally pure, i.e., having no other line within ±0.1 nm, are shortlisted. Among these emission lines, only those lines that have ~10–15 pixels as a part of the background at the right or left of the peak are selected. These 10–15 pixels are used for the noise calculation. Among these, only two emission lines that have the best emission intensity are selected (one from each element, Cr and Ni). In the present study, these emission lines are Cr(I) 435.17 nm and Ni(I) 351.50 nm.

Optimization of analytical parameter. To study the effect of both independent experimental parameters, the signal-to-noise ratio was measured by varying the acquisition time delay at a particular laser energy value. Figure 1 shows a three-dimensional plot of the laser energy vs. acquisition time delay vs. signal-to-noise ratio for Cr(I) 435.17 nm. In Fig. 1, it can be seen that the signal-to-noise ratio of Cr(I) 435.17 nm generally increases with increasing laser energy and decreasing acquisition time delay. In the experimental condition zone of ≥0.5 and acquisition time delay ≥2 μs, the LIBS signal increases monotonically, thereby causing an increase in the signal to noise ratio with the laser energy until the plasma density becomes too high at the laser energy of ~80–95 mJ. The excitation temperature and electron number density determined by the method described by Ley et al. for the analysis condition of 30 mJ laser energy and 1 μs acquisition delay were 8000 K and 0.8×10^{16} cm^{-3}, respectively [21]. At 90 mJ laser energy and 1 μs acquisition delay they increase to 12,000 K and 2.5×10^{16} cm^{-3}. At still higher laser energy (>95 mJ), probably due to the shielding of laser light, the analyte signal starts decreasing, causing a reduction in the signal to noise ratio parameter. At 130 mJ laser energy and 1 μs acquisition delay, the electron excitation

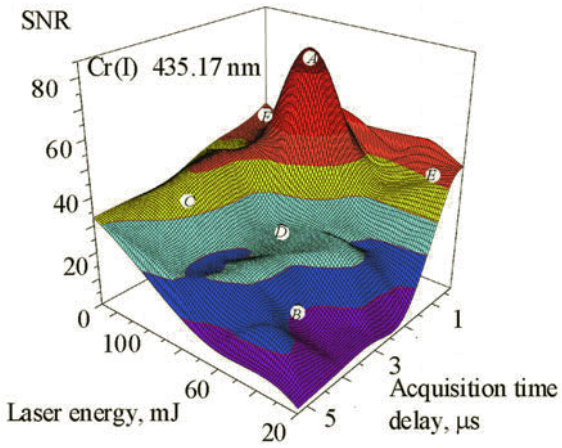

Fig. 1. Variation of signal to noise ratio of Cr(I) 435.17 nm with laser energy and acquisition time delay. White circles indicate different experimental conditions used in the study for evaluating their effect on the LIBS analytical performance for Cr quantification.

temperature and electron number density were found to be highest among various experimental conditions used in the study (16000 K and 4.5×10^{16} cm^{-3}). The ignal to noise ratio was found to be the highest at the acquisition time delay of 0.85–1.25 μs for the laser energy of 80–95 mJ. Hence, the laser energy of 90 mJ and the acquisition time delay of 1.1 μs are chosen as optimum analysis conditions for Cr in a steel matrix. Similar experiments with Ni(I) 351.50 nm showed that the optimum laser energy is 95 mJ and the acquisition time delay is 1.3 μs.

Choice of experimental conditions. Since the goal of the study was to evaluate the effect of different experimental conditions on analytical performance of LIBS, apart from the optimized condition for Cr and Ni analysis, five additional experimental conditions were also selected for the LIBS analysis. These experimental conditions are shown in Fig. 1 as white circles. The experimental conditions were chosen in such a way that the experimental variable field can be evaluated with these conditions. The experimental condition A represents the optimum experimental condition for Cr and Ni in the respective analysis. The condition B represents the condition of low laser energy but high acquisition delay (45 mJ and 3.5 μs). The condition C represents high laser energy with high acquisition delay condition (110 mJ and 4 μs). The condition D was chosen in such a way that it represents a medium laser energy and acquisition delay condition but away from the optimum experimental condition (70 mJ and 2.5 μs). The condition E on the other hand, represents the situation of low laser energy (30 mJ) along with a relatively low acquisition delay (0.8 μs). Lastly, the experimental condition F represents the condition of high laser energy accompanied by small acquisition delay (125 mJ and 0.4 μs). No condition having acquisition delay more than 4 μs was selected, as the signal to noise ratio was negligibly small in that region.

Analytical performance. In PLSR, before calibration, optimization of the number of factors (which is equivalent to the principal components in principal component regression) is carried out in order to avoid overfitting. This has been performed by applying a cross-validation method to calculate the root mean square error of calibration (RMSEcv). These values were different for Ni and Cr and also different in different experimental conditions, as indicated in Table 2. It was found that irrespective of the experimental condition, R^2 of the PLSR calibration curves is ~1. But the RMSECcv reveals that the experimental condition A is the best condition and B is the worst, whereas there is not much to distinguish between the other experimental parameters. But since the true quality of PLSR models is unknown, they can only be judged by comparing their prediction quality, i.e., SEP of these models. SEP is a type of mean square error and hence has two components. One measures the variability of the estimator, i.e., precision, and the other measures the bias or accuracy. Figure 2 give details of the SEP determined at different experimental conditions for Cr and Ni. It can be seen from these two figures that the least SEP is obtained at the optimum experimental conditions of the respective elements, i.e., at the condition A. As one deviates from the optimum condition in any direction of laser energy or acquisition time delay axis, the SEP increases, indicating a decrease in accuracy and precision. The SEP values of Cr (0.9) and Ni (1.7) in the optimum condition are similar to the values 0.5 and 0.7, respectively, obtained by the principal component regression method of Zaytsev et al. [22]. This result can be attributed to the fact that as we move from the optimum experimental condition, we are also shifting to the position of a poorer signal-to-noise ratio.

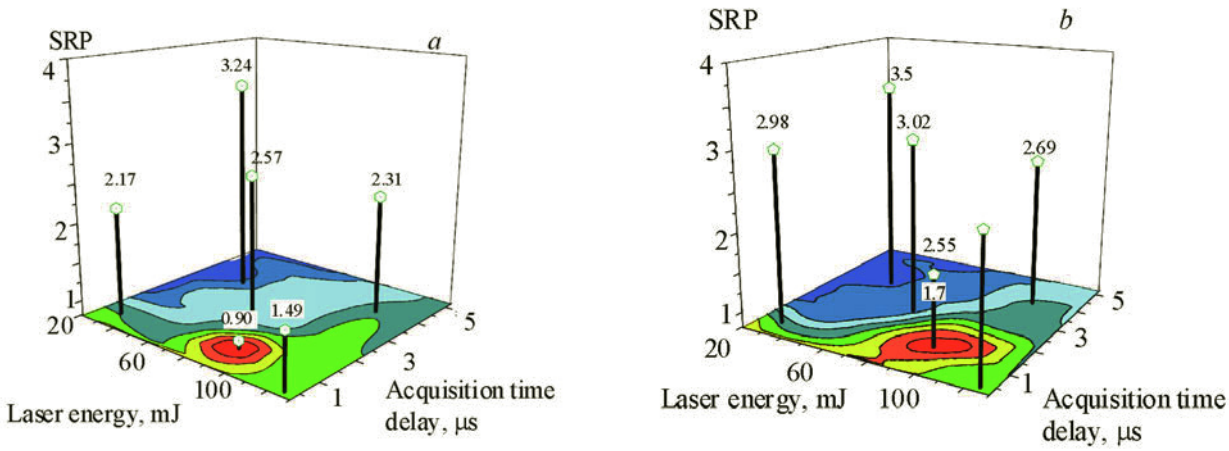

Fig. 2. Standard error of prediction determined at different experimental conditions for quantification of Cr (a) and Ni (b) in steel.

TABLE 2. Different Parameters of Partial Least Squares Regression Calibration at Different Experimental Conditions for Cr and Ni

Condition	Factor used in PLSR calibration		R^2		RMSECcv	
	Cr	Ni	Cr	Ni	Cr	Ni
A	6	6	0.9999	0.9999	0.3264	0.1849
B	7	7	0.9992	0.9996	0.5983	0.4445
C	6	6	0.9998	0.9993	0.4598	0.3016
D	6	7	0.9990	0.9991	0.4405	0.3532
E	8	8	0.9994	0.9981	0.4147	0.3621
F	4	6	0.9994	0.9992	0.4409	0.3326

It is interesting to note that the conditions E and C, which are completely opposite to each other, generate similar signal-to-noise ratio. In the condition C a high value of laser energy produces high signal and noise ratio, but a high acquisition time delay reduces the continuum emission, thereby the corresponding noise, generating a signal-to-noise ratio of ~35. Whereas in the condition E a low acquisition time delay yields a very hot plasma and hence a strong signal, a low laser energy means less ablation of materials in the plasma, which compensates the effect of low acquisition delay and generates a signal to noise ratio of ~34.

Figure 3 shows the effect of different experimental conditions on the signals of Cr(I) 435.17 nm and Ni(I) 351.50 nm. Figure 3 clearly demonstrates that the conditions C and E generate almost similar signal and noise (visible from the random fluctuation of the background point adjacent to the peak) for Cr(I) 435.17 nm. Though the two conditions E and C are poles apart from each other, they generate similar signal-to-noise ratio. The SEP at these two conditions for both Cr (SEP = 2.31 and 2.17) and Ni (SEP = 2.69 and 2.98) is practically the same. The experimental condition F was found to generate the most intense signal. But it is also associated with very strong noise at the peak base, as visible in Fig. 3. The worst among these six conditions, was the condition B, as expected, due to the use of low laser energy and high acquisition time delay, causing a drastic reduction in the Cr/Ni signal. The experimental condition A, which is the optimum condition was found to generate a strong signal accompanied by a low noise contribution. Spectroscopic diagnostic information (electron excitation temperature and electron number density) on the plasma at these six experimental conditions was also determined as described previously. It was interesting to find out that the plasma was in local thermodynamic equilibrium only in the condition A and F, as per the McWhirter criterion [23].

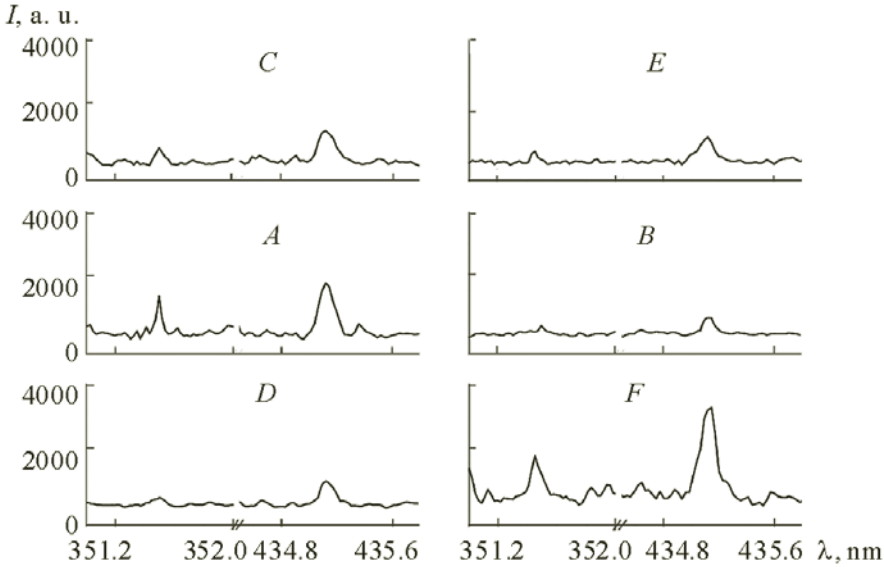

Fig. 3. Spectral profiles of Cr(I) 435.17 nm and Ni(I) 351.50 nm at different experimental conditions A–F.

The magnitude of SEP is a concentration-dependent parameter. Analytical scientists prefer concentration-independent parameters like percentage accuracy and relative standard deviation (RSD) to evaluate the analytical performance. For 10 replicates, analyses of the three validation set samples using PLSR algorithm in six different experimental conditions for Cr in steel show the best analytical performance at the condition A.

An accuracy of 2.5–3% and RSD of 3.5–5% was obtained in the experimental condition A. Similar results were also obtained for Ni, with accuracy of 5–8% and RSD of 7–9% at the experimental condition A for the three validation set samples. It can be seen from Figs. 1–3 and the analytical results that the best results in terms of either SEP or accuracy or precision were obtained only with the optimum experimental parameter setting. This clearly shows the importance of optimizing experimental conditions in LIBS to achieve the best possible analytical results.

Conclusions. Laser-induced breakdown spectroscopy was applied for evaluating the effect of different experimental conditions, namely, the laser energy and the acquisition time delay on the overall analytical performance of the LIBS analyses of Cr and Ni in steel. The analyses were carried out by using the PLSR algorithm. The optimum condition for the analysis based on the signal to noise ratio parameter was found to be nearly the same for both elements with laser energy of 90–95 mJ and acquisition delay of 1.1–1.3 μs. Five more different experimental conditions using several combinations of laser energy and acquisition time delay were also used for the LIBS study. It is observed that the least SEP is obtained at the optimum experimental conditions of the analysis. With a deviation from the optimum condition in any direction of either laser energy or acquisition time delay axis, the SEP increases, indicating a decrease in accuracy and precision, i.e., a poorer analytical performance. The results show that the signal-to-noise ratio and SEP are correlated to each other in an inverse manner. It was also observed that, when two conditions, which are completely different, produce similar signal-to-noise ratio values, the analytical performance will also be similar. The results in terms of accuracy and precision were also found to be best in the optimized experimental conditions for both Cr and Ni. The study demonstrates the need and importance of selecting optimum experimental parameters, namely, laser energy and acquisition time delay in LIBS, to achieve the best possible analytical results, i.e., accuracy and precision.

Acknowledgments. The authors are thankful to D. Alamelu, Head, Mass Spectrometry Section, S. Kannan, Head, Fuel Chemistry Division, Prof. B. S. Tomar, Associate Director, Radiochemistry and Isotope Group, and Prof. K. L. Ramakumar, Director, Radiochemistry and Isotope Group, B.A.R.C. for their constant support and encouragement in the LIBS work.

REFERENCES

1. G. C. Dacey, *Science*, **135**, 71–74 (1962).
2. A. E. Pichahchy, D. A. Cremers, and M. J. Ferris, *Spectrochim. Acta B*, **52**, 25–39 (1997).

3. B. Sallé, D. A. Cremers, S. Maurice, and R. C. Wiens, *Spectrochim. Acta B*, **60**, 479–490 (2005).
4. S. Qiao, Y. Ding, D. Tian, L. Yao, and G. Yang, *Appl. Spectrosc. Rev.*, **50**, 1–26 (2015).
5. F. J. Fortes, J. Moros, P. Lucena, L. M. Cabalin, and J. J. Laserna, *Anal. Chem*., **85**, 640–669 (2013).
6. J. P. Singh and S. N. Thakur, *Laser-Induced Breakdown Spectroscopy*, Elsevier, Amsterdam (2007).
7. R. Noll, *Laser-Induced Breakdown Spectroscopy: Fundamentals and Applications*, Springer, New York (2012).
8. A. Sarkar, K. Sasibhusan, D. Alamelu, and S. K. Aggarwal, *Laser Eng.*, **26**, 137–146 (2013).
9. A. Sarkar, R. K. Mishra, C. K. Kaushik, P. K. Wattal, D. Alamelu, and S. K. Aggarwal, *Radiochim. Acta*, **102**, 805–812 (2014).
10. A. N. Kadachi and M. A. Al-Eshaikh, *Spectrosc. Lett.*, **48**, 403–410 (2015).
11. V. Majidi and M. R. Joseph, *Crit. Rev. Anal. Chem.*, **23**, 143–162 (1992).
12. D. W. Hahn and N. Omenetto, *Appl. Spectrosc*., **64**, 335–366 (2010).
13. A. Sarkar, V. M. Telmore, D. Alamelu, and S. K. Aggarwal, *J. Anal. At. Spectrom*., **24**, 1545–1550 (2009).
14. D. A. Cremers and L. J. Radziemski, *Handbook of Laser-Induced Breakdown Spectroscopy*, John Wiley & Sons, Ltd., Chichester, West Sussex, UK (2006).
15. R. Wisbrun, I. Schechter, R. Niessner, H. Schroeder, and K. L. Kompa, *Anal. Chem.*, **66**, 2964–2975 (1994)
16. C. B. Stipe, B. D. Hensley, J. L. Boersema, and S. G. Buckley, *Appl. Spectrosc.*, **64**, 154–160 (2010).
17. A. Sarkar, V. Karki, S. K. Aggarwal, G. S. Maurya, R. Kumar, A. K. Rai, X. Mao, and R. E. Russo, *Spectrochim. Acta B*, **108**, 8–14 (2015).
18. R. G. Brereton, *Analyst,* **125**, 2125–2154 (2000).
19. M. C. Ortiz, L. Sarabia, A. Jurado-López, and M. D. Luque de Castro, *Anal. Chim. Acta*, **515**, 151–157 (2004).
20. www.pmp.uni-hannover.de/cgi-bin/ssi/test/kurucz/sekur.html.
21. H. Ley, A. Yahaya, and R. Ibrahim, *J. Sci. Technol*., **6**, 49–66 (2014).
22. S. M. Zaytsev, A. M. Popov, E. V. Chernykh, R. D. Voronina, N. B. Zorov, and T. A. Labutin, *J. Anal. At. Spectrom.*, **29**, 1417–1424 (2014).
23. G. Cristoferetti, A. De Giacomo, M. Dell'Aglio, S. Legnaioli, V. Palleshi, and N. Omenetto, *Spectrochim. Acta B*, **65**, 86–95 (2010).